RESEARCH PAPER

Nano Science and Technology Journal 1(1) 1-16 Summer 2023

Pentetic Acid-Copper Complex-Functionalized Magnetite Nanoparticles: An Efficient and Magnetically Separable Catalyst for Solvent-Free Synthesis of Benzimidazoles

Hassan Moghanian*[1], Mohamad Naseh[1]

[1]*Department of Chemistry, Dezful Branch, Islamic Azad University, Dezful, Iran*

Article History:
Received 05 August 2023
Accepted 08 September 2023
Published 22 September 2023

Keywords:
Benzimidazole
Magnetic nanoparticles,
Pentetic acid-copper complex
Heterogeneous catalyst
Solvent-free

*Corresponding Authors Email:
moghanian@gmail.com

DOI: 10.22034/nstj.2023.707459

Abstract

This paper presents the synthesis of a novel magnetically heterogeneous nanocatalyst, MNPs-DTPA-Cu, which is composed of Fe_3O_4 nanoparticles modified with a copper complex of pentetic acid or diethylenetriaminepentaacetic acid (DTPA). The synthesis process involves a simple and cost-effective two-step procedure using readily available precursors. The structure of these nanoparticles was characterized using several techniques, including SEM, TGA, XRD, FTIR, VSM, EDS. These techniques provided valuable insights into the composition and properties of the nanoparticles. The catalytic performance of this novel material has been thoroughly investigated in the synthesis of benzimidazole derivatives through a one-pot condensation reaction of aldehydes and o-phenylenediamine. Remarkably, the reaction proceeded under solvent-free classical heating conditions, resulting in good to excellent yields of the desired products. The present catalytic system possesses several notable features, including shorter reaction time, mild reaction conditions, simplicity, and non-toxicity. Additionally, the catalyst can be easily recovered using an external magnet and can be reused up to six consecutive times without any significant loss in catalytic efficiency.

1. Introduction

Benzimidazoles and their derivatives belong to a class of nitrogen-containing heterocycles that play a crucial role as structural scaffolds. These compounds are widely utilized in drug development and material design due to their remarkable pharmacological and biological properties [1,2]. They possess a wide array of applications, encompassing antiviral, anti-inflammatory, antidepressant, antitumor, antifungal, antimycotic, antibiotic, antiulcerative, antibacterial, and anti-allergic properties (Fig. 1) [3-5].

The development of compound libraries derived from benzimidazoles has garnered significant attention due to their exceptional therapeutic applications. Researchers have dedicated substantial efforts to explore various synthetic schemes for these compounds, involving the reaction between *o*-phenylenediamine and carboxylic acid or its derivatives, such as nitriles, amides and orthoesters [6]. Conventionally, these reactions occur under harsh dehydrating

conditions. However, one technique has emerged as the most efficient and widely employed in this field: the condensation of *o*-phenylenediamine with aldehydes [7]. This method comprises two distinct steps: the initial formation of a Schiff's base, followed by oxidative cyclocondensation. A literature survey reveals that a wide range of catalysts have been employed in the condensation reaction between o-phenylenediamines and aldehydes. These catalysts include: $FeCl_3.6H_2O$ [8], $In(OTf)_3$ [9], $Cu(OTf)_2$ [10], $ZrOCl_2.8H_2O$ [11], Au/CeO_2 [12], $I_2/KI/K_2CO_3/H_2O$ [13], sodium metabisulfite [14], silica sulfuric acid [15] and iodobenzene diacetate [16].

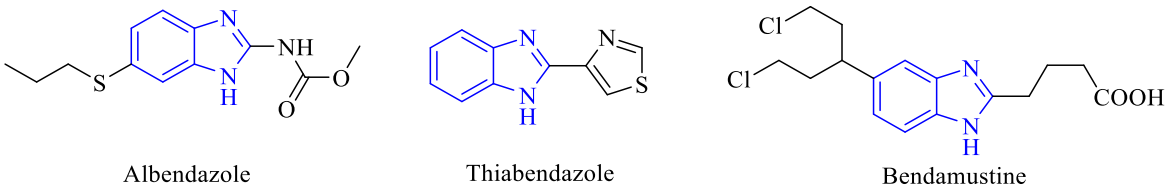

Fig. 1. Examples of bioactive benzimidazoles.

Although these methods may be applicable under certain synthesis conditions, they often suffer from several drawbacks. These drawbacks include prolonged reaction times, elevated reaction temperatures, low yields of the desired product, tedious work-up procedure, toxicity concerns, and limited catalyst recovery and reusability. As a result, there is a pressing need for the development of an efficient and mild method that can effectively overcome these limitations.

In response to the escalating concern about the environmental effects of organic solvents, synthetic chemists have shifted their focus towards employing chemical reactions that eliminate the requirement for traditional organic solvents. This approach has proven to be an efficient technique in numerous organic reactions. Solvent-free conditions have consistently demonstrated notable benefits, including reduced reaction time, increased yield, simplified product separation, and, in certain instances, enhanced selectivity in stereochemistry [17].

In recent decades, the advancement of green chemistry has led to a significant interest among scientists in the synthesis and application of magnetic nanoparticles (MNPs) as catalysts [18-21]. One of the notable advantages of these nanocatalysts is their convenient separation using an external magnet, eliminating the requirement for filtration. This characteristic simplifies the catalyst recovery process and enhances the overall efficiency of the system. However, due to spontaneous interactions, magnetic nanoparticles tend to aggregate rapidly. To overcome this drawback, the surface of MNPs is frequently modified by capping them with specific layers, such as organic ligands, organic-inorganic hybrids, and inorganic nanoparticles [22-24]. This crucial step facilitates the appropriate dispersion and shields the iron nanoparticles from environmental factors, including oxidation.

In this report, we present the preparation of a novel magnetic nanocatalyst through the immobilization of a pentetic acid-copper complex on Fe_3O_4 nanoparticles. This catalyst exhibits remarkable potential as cost-effective, highly efficient, and magnetically recoverable solution for the one-pot synthesis of benzimidazole derivatives under solvent-

free conditions. The method proved to be highly advantageous, owing to the catalyst's noteworthy efficiency and its environmental compatibility.

2. Materials and methods

Reagents were purchased from Sigma Aldrich and Merck Chemical Co. and used without further purification. Fourier transform infrared (FT-IR) spectra were recorded on a Unicom Galaxy Series FT-IR 5000 spectrophotometer with a scanning range of 4000-400 cm^{-1} at a resolution of 2 cm^{-1}, using pressed KBr discs. Melting points were determined using capillary tubes on an electrothermal digital apparatus and are reported as uncorrected values. Thin layer chromatography (TLC) was employed to monitor the progress of reactions, with the eluent being *n*-hexane/EtOAc. ^{1}H NMR (300 MHz) spectra were recorded in DMSO-d_6 on a Bruker Avance instrument. X-ray diffraction (XRD) of the catalyst was performed using a Philips X-3064 Pert Pw (Cu kα radiation, λ=1.54 Å) in the 2Θ range of 20°- 80°. The particle size and external morphology, as well as the elements of MNPs-DTPA-Cu, were analyzed using a Hitachi S-4700 field emission-scanning electron microscope (FE-SEM) and energy-dispersive X-ray spectroscopy (EDS) analysis. Thermal gravimetric analysis (TGA) and differential thermal gravimetric (DTG) were conducted from 50 °C to 700 °C, with a heating rate of 10 ºC/min, under a nitrogen atmosphere using a TA Instruments TGAQ5000.

Preparation of the magnetic Fe_3O_4 nanoparticles (MNPs)

The synthesis of Fe_3O_4-MNPs was accomplished through a well-established chemical co-precipitation technique, as documented in the relevant literature [25]. Briefly, a mixture of $FeCl_3.6H_2O$ (10 mmol, 2.703 g) and $FeCl_2.4H_2O$ (5 mmol, 0.994 g) was introduced into a 250 mL flask, followed by the addition of approximately 100 mL of double-distilled water. The mixture was then heated at 80°C for 1 hour under a nitrogen atmosphere. Subsequently, 10 mL of a 25% ammonia solution was carefully added to the flask contents, and the reaction mixture was stirred at 80°C for 30 minutes. The black precipitate formed was effectively separated from the reaction mixture using a powerful magnet. The resulting nanoparticles were thoroughly washed with double-distilled water until reaching a neutral pH, followed by additional washing with ethanol. Finally, the nanoparticles were dried at 80°C under vacuum.

Synthesis of pentetic acid-Copper complex -functionalized magnetic nanoparticles (MNPs-DTPA-Cu)

In a meticulous experimental procedure, 0.098 grams of pentetic acid (0.25 mmol), along with an equivalent amount of $Cu(NO_3)_2{\cdot}3H_2O$ (0.25 mmol, 0.060 g), were dissolved in 10 mL of ammonia solution and stirred for a duration of 2 hours at room temperature. Subsequently, the resulting solution was introduced into a blend of uniformly dispersed magnetic nanoparticles (MNPs), weighing 0.5 gram, in 100 mL of deionized water. The reaction mixture was subjected to reflux for a period of 6 hours, all while maintaining a nitrogen atmosphere. Following the reflux process,

the resulting black precipitate (MNPs-DTPA-Cu) was washed from the solution using a magnet, and subsequently rinsed multiple times with water and ethanol. Finally, the precipitate was dried under vacuum conditions at a temperature of 25°C.

General Procedure for the Synthesis of benzimidazole derivatives

A catalyst of MNPs-DTPA-Cu (0.05 g) was added to a mixture containing 1 mmol of aldehyde and 1 mmol of *o*-phenylenediamine. The mixture was stirred using a magnetic stirrer under thermal solvent-free conditions on a preheated oil bath at 80°C for the appropriate duration. Once the reaction was complete, as confirmed by TLC analysis, the resulting solidified mixture was diluted with 10 mL of hot ethanol. The catalyst was easily separated from the mixture using an external magnet. The solvent was then evaporated, leaving behind a solid product which was subsequently recrystallized from aqueous ethanol.

Characterization data for selected compounds:

2-phenyl-1H-benzo[d]imidazole (3**a**):

IR (KBr): ν_{max} = 3054, 3018, 2976, 1463, 1448, 1416, 1280, 1069, 971, 744, 704, 690 cm^{-1}; ^1H NMR (300 MHz, DMSO-d_6): δ = 12.13 (s, 1H), 8.26 (t, J = 8 Hz, 2H), 7.71-7.53 (m, 5H), 7.20 (s, 2H).

2-(4-chlorophenyl)-1H-benzo[d]imidazole (**3b**):

IR (KBr): ν_{max} = 30419, 3081, 2962, 1600, 1491, 1475, 1438, 1322, 1274, 1120, 1097, 1069, 838, 761, 741, 690 cm^{-1}; ^1H NMR (300 MHz, DMSO-d_6): δ = 13.05 (s, 1H), 8.18 (d, J = 7.9 Hz, 2H), 7.60-7.55 (m, 2H), 7.50 (d, J = 8 Hz, 2H), 7.20-7.16 (m, 2H);

3. Results and discussion

Synthesis and characterization of the catalyst

In this study, MNPs-DTPA-Cu nanoparticles were synthesized through a straightforward two-step method outlined in Scheme 1. Initially, we synthesized magnetite (Fe_3O_4) nanoparticles by co-precipitation from a solution containing iron (II) and iron (III) salts, with ammonia serving as the precipitating agent. The magnetite nanoparticles were subsequently subjected to a sequential treatment involving a solution containing pre-mixed pentetic acid (DTPA) and copper (II) salt in ammonia. This treatment aimed to establish covalent bonds between the hydroxyl (OH) groups present on the particle surface and the DTPA-Cu (II) complex. It is noteworthy that DTPA, when complexed with

copper (II), exhibits a hexadentate binding mode [26]. This binding mode efficiently utilizes three amine centers and three out of the five carboxylate groups.

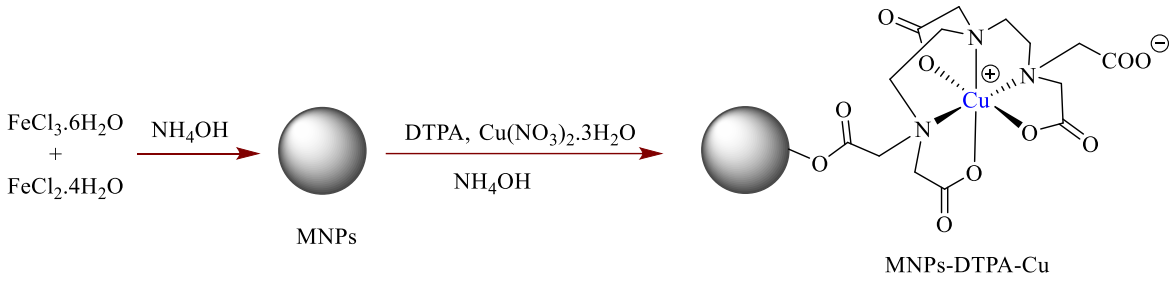

Scheme 1. Synthesis of MNPs-DTPA-Cu nanoparticles.

To characterize the structure, size, and morphology of the magnetite nanocatalyst (MNPs-DTPA-Cu), a range of analytical techniques were employed. These techniques included infrared spectroscopy (IR), thermal analysis (TG), X-ray diffraction (XRD), scanning electron microscopy (SEM), and vibrating sample magnetometry (VSM).

Figure 2 displays the FT-IR spectra of Fe_3O_4 and MNPs-DTPA-Cu nanoparticles within the wavenumber range of 4000-400 cm^{-1}. The FT-IR spectra of these compounds align with the Fe_3O_4 materials previously documented in the literature. As observed in the infrared spectrum of Fe_3O_4 (Figure 2a), the stretching vibrations related to Fe-O bonds appear at 578 cm^{-1}. Furthermore, the broad peak detected in the 3450 cm^{-1} region corresponds to the stretching vibrations of surface hydroxyl groups. Additionally, the presence of a weak absorption at 1620 cm^{-1} can be attributed to the bending vibrations of H-O-H, which are absorbed on the surface of the nanoparticle.

The FT-IR spectrum of MNPs-DTPA-Cu (Figure 2b) displays absorption bands at 1639, 1560, and 1412 cm^{-1}. These bands are assigned to the asymmetric and symmetric stretching modes of the carboxylate groups. Additionally, the bands observed at 1339 and 1021 cm^{-1} can be attributed to the stretching vibrations of C-N and C-O bonds in MNPs-DTPA-Cu, respectively. On the other hand, the weak absorption bands at 2960 and 2922 cm^{-1} are assigned to the symmetric and asymmetric stretching vibrations of aliphatic CH_2 groups. These findings provide evidence of the successful functionalization of the surface of Fe_3O_4 nanoparticles with the DTPA-Cu (II) complex.

A field emission scanning electron microscopy (FE-SEM) image of MNPs-DTPA-Cu nanoparticles is presented in Figure 3, offering valuable insights into the morphological characteristics and particle size of these nanoparticles. The FE-SEM image clearly depicts that the nanoparticles retain their nearly spherical three-dimensional shape, with a size below 75 nanometers. This particular particle size is believed to enhance the catalyst's interaction with the reactants, thereby leading to a favorable yield of the desired product.

Figure 4 shows the EDS spectrum and X-ray map of the magnetite MNPs-DTPA-Cu nanoparticles, providing valuable insights into the composition of the sample. The presence of Cu signals within the energy range of 8.16 keV and 0.85 keV in the EDS spectrum clearly indicates the successful functionalization of Fe_3O_4 nanoparticles with the DTPA-Cu

(II) complex. Furthermore, the EDS spectrum of the catalyst reveals the presence of Fe, N, O, and C elements, confirming the effective coating of the magnetite nanoparticle with the pentetic acid-copper complex. These findings serve as concrete evidence of the successful synthesis of the nanoparticles. Moreover, the map spectrum visually demonstrates the uniform dispersion of MNPs-DTPA-Cu nanoparticles within the Fe_3O_4 matrix, with minimal agglomeration.

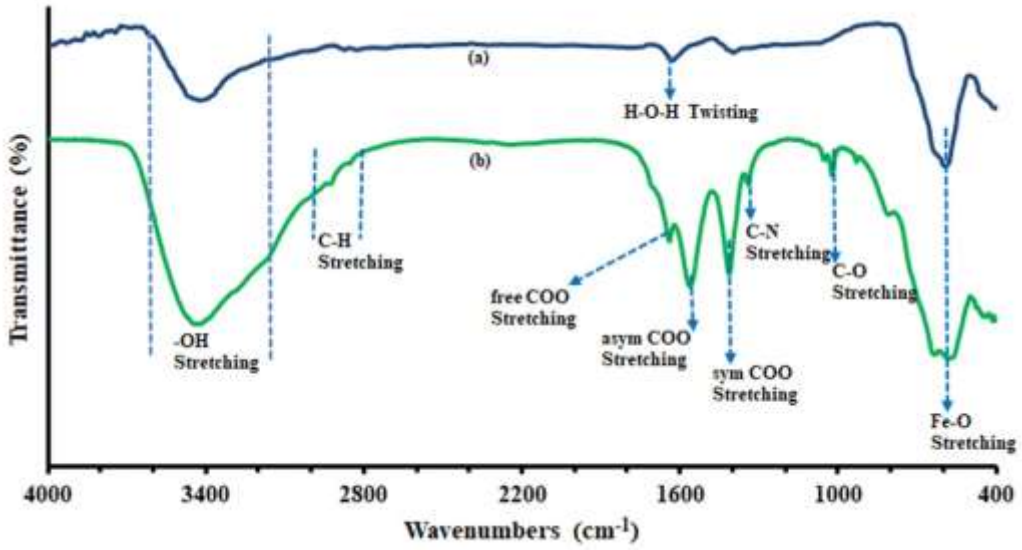

Fig. 2. The comparative FT-IR spectra for (a) Fe_3O_4, (b) MNPs-DTPA-Cu nanoparticles.

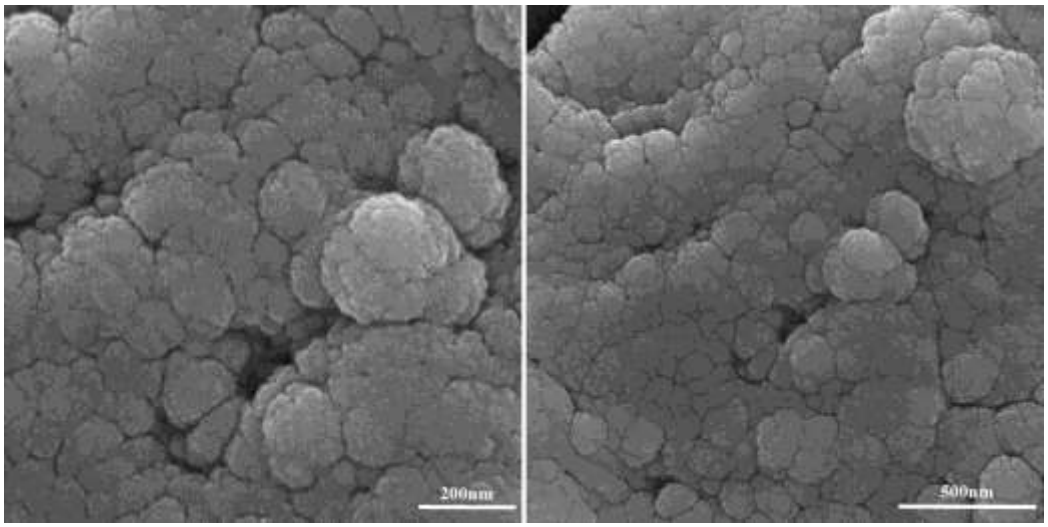

Fig. 3. FE-SEM images of MNPs-DTPA-Cu nanoparticles.

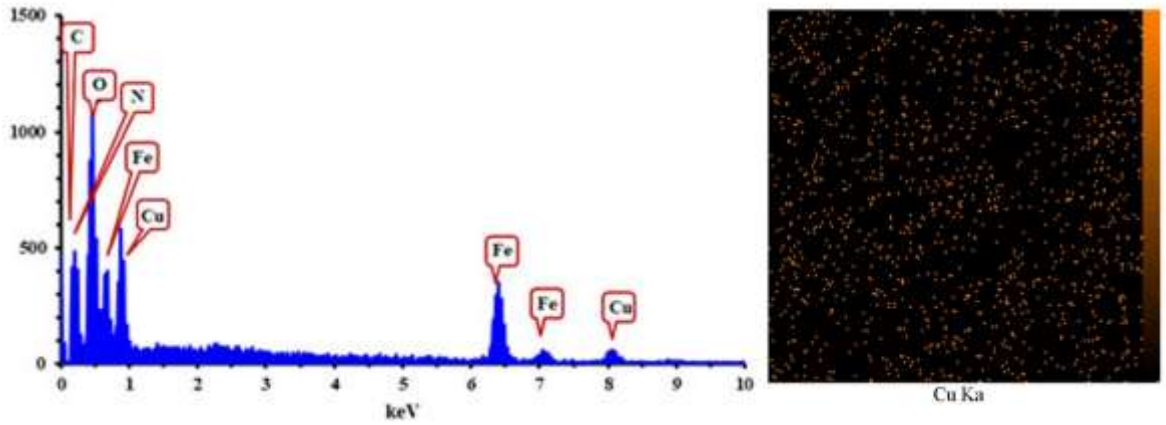

Fig. 4. The EDS spectrum and X-ray map of MNPs-DTPA-Cu nanoparticles.

The crystallographic and phase analysis of the synthesized MNPs-DTPA-Cu nanoparticles was conducted using X-ray diffraction (XRD) analysis. Figure 5 displays the XRD pattern of the prepared nanoparticles. By comparing it to the standard pattern (JCPDS card No. 85-1436), which represents the crystal structure of pure Fe_3O_4 with a cubic spinel structure, we can confirm the excellent crystallinity of the prepared samples during the coating stages, as evidenced by the sharp crystalline peaks. The XRD pattern of the synthesized particles reveals the presence of seven distinct diffraction peaks at angles of 30.3º, 35.6º, 43.2º, 53.7º, 57.2º, 63.2º, and 74.4º for 2θ. These peaks correspond to the planes (220), (311), (400), (422), (511), (440), and (533) in the Fe_3O_4 nanoparticles. Significantly, the absence of impurities in the XRD patterns confirms the formation of pure MNPs-DTPA-Cu nanoparticles.

The average size of the magnetic nanoparticles' crystallites was determined by employing the Scherrer's equation ($D = 0.9\ \lambda/\beta\ \cos\theta$), with the (311) peak in the X-ray diffraction (XRD) pattern serving as a reference. In this equation, D represents the average crystallite size, λ denotes the X-ray wavelength (0.154 nanometers), β signifies the peak width at half-maximum intensity of the (311) peak in radians, and θ represents the Bragg angle of the (311) peak in degrees [27]. Utilizing this equation, the calculated average crystallite size of the magnetic nanoparticle is approximately 54 nanometers.

The thermal stability of MNPs-DTPA-Cu was investigated through thermogravimetric analysis (TGA) and derivative thermogravimetry (DTG), with the results depicted in Figure 6. The TGA curve of the MNPs-DTPA-Cu catalyst displayed two distinct decomposition stages. According to the TGA curve, the mass loss of MNPs-DTPA-Cu nanoparticles up to 300°C can be attributed to the release of adsorbed solvents and surface hydroxyl groups. Subsequently, a significant weight loss between approximately 400-650 °C is associated with the evaporation and disintegration of organic groups grafted onto the surface of MNPs-DTPA-Cu.

By analyzing the mass loss observed during the second decomposition stage, it was determined that 0.41 mmol of DTPA-Cu (II) complex was loaded onto 1 g of MNPs- Furthermore, the DTG curve demonstrates that the organic

structure decomposes predominantly in a single step, ranging from 450 °C to 650 °C. Consequently, it can be inferred that the MNPs-DTPA-Cu catalyst maintains its stability at temperatures up to or below 300 °C.

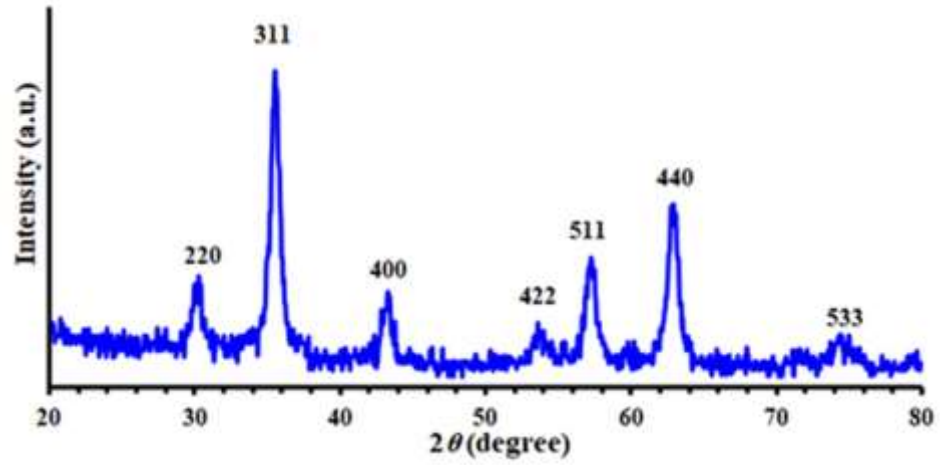

Fig. 5. XRD diffraction pattern of MNPs-DTPA-Cu nanoparticles.

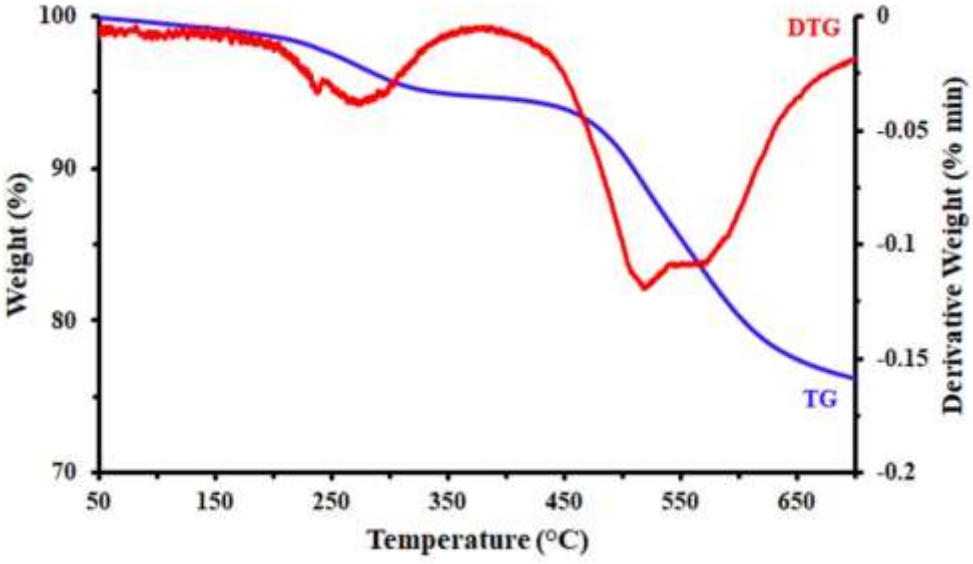

Fig. 6. TG-DTG analyses of MNPs-DTPA-Cu nanoparticles.

In order to evaluate the magnetic properties of MNPs-DTPA-Cu nanoparticles, a vibration sample magnetometer (VSM) was employed at room temperature (Fig. 7). Hysteresis curves were utilized to extract significant information regarding the saturation magnetization (Ms), residual magnetization (Mr), and coercive magnetic field (Hc). These parameters play a vital role in understanding the magnetic behavior of the nanoparticles.

Based on the data presented in Figure 7, the saturation magnetization value of the synthesized catalyst was determined to be 39.2 emu/g. This value is significantly lower than the saturation magnetization of the neat Fe_3O_4 magnetic nanoparticles, which were measured at 60 emu/g. The observed difference can be attributed to the surface coverage of the Fe_3O_4 magnetic nanoparticles by the DTPA-Cu (II) complex.

The size of ferromagnetic particles plays a crucial role in determining their magnetic properties [28]. The MNPs-DTPA-Cu nanoparticles, as depicted in Figure 7 (left inset), exemplify superparamagnetic characteristics with low residual magnetization and a coercive magnetic field. Moreover, these nanoparticles demonstrate remarkable magnetization and have a tendency to aggregate when subjected to an external magnet. They quickly form clusters under the magnetic field and disperse effortlessly upon its removal. This distinctive behavior can be attributed to their exceptional magnetic properties.

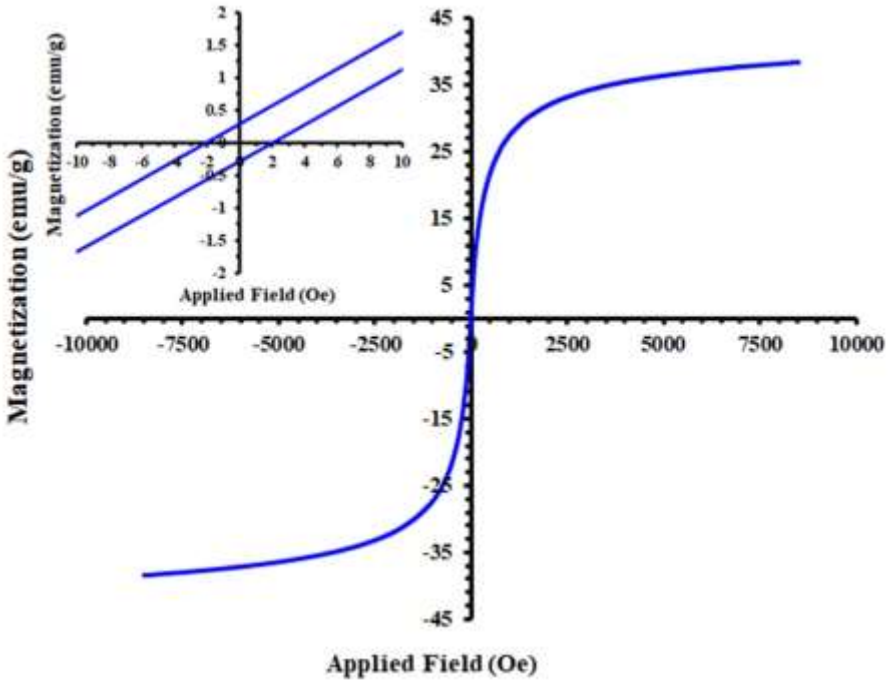

Fig. 7. The magnetic hysteresis loops of MNPs-DTPA-Cu. Left inset: the magnified field from -10 to 10 Oe.

Synthesis of benzimidazole derivatives using MNPs-DTPA-Cu

Once the structure of the MNPs-DTPA-Cu catalyst was determined, our attention turned to assessing its catalytic performance in the synthesis of benzimidazole derivatives (Scheme 2). One notable feature of these nanocatalysts is their convenient separation through the application of an external magnetic field, thereby eliminating the requirement for filtration or centrifugation.

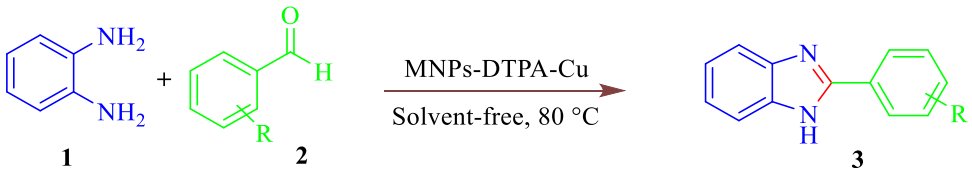

Scheme 2. Synthesis of benzimidazole derivatives.

In order to enhance the reaction conditions and achieve the best catalyst activity, we employed the reaction between benzaldehyde (1 mmol) and *o*-phenylenediamine (1 mmol) as a model.

The reaction was then carried out using a variety of solvents, different temperatures and even under solvent-free conditions, aiming to attain a satisfactory product yield. Initially, a range of solvents such as ethyl acetate, acetonitrile, ethanol, toluene, *n*-hexane, and water were utilized under various conditions. Regrettably, these solvents yielded unsatisfactory outcomes, and the reaction time was also significantly prolonged in these cases (Table 1). The assessment of the reaction, employing different solvents, has revealed that conventional heating at 80°C without the use of solvents is the preferred method due to its remarkable efficiency and environmental compatibility (Table 1, entry 9).

Additionally, we have successfully optimized the quantity of catalyst employed in the experiment. In the absence of the MNPs-DTPA-Cu catalyst, the majority of the initial materials remained unchanged and no product was formed (Table 1, entry 13). However, upon the introduction of the catalyst, it exhibited remarkable performance in producing the desired product. Based on the data presented in Table 1, it is clear that increasing the catalyst amount to 0.1 grams did not lead to a significant alteration in the reaction outcome. However, when the catalyst amount was reduced to 0.02 grams, a noticeable decrease in the reaction yield was observed.

As a final outcome, as shown in Table 1, the utilization of a 0.05 grams catalyst at a temperature of 80°C, under solvent-free conditions, had a significant impact on the efficiency of producing benzimidazole derivatives. This process achieved an impressive yield of 94% (Table 1, entry 9).

Table 1. Oxidative condensation of *o*-phenylenediamine (1 mmol) and benzaldehyde (1 mmol) in the presence of MNPs-DTPA-Cu under different conditions.

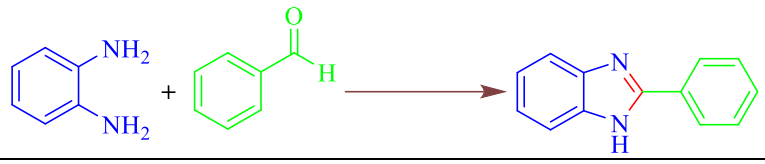

Entry	Catalyst (g)	Solvent	Condition	Time	Yield (%)[a]
1	MNPs-DTPA-Cu (0.05)	EtOH	R.T.	12 h	15
2	MNPs-DTPA-Cu (0.05)	EtOH	Reflux	3 h	40
3	MNPs-DTPA-Cu (0.05)	EtOAc	Reflux	3 h	50
4	MNPs-DTPA-Cu (0.05)	Toluene	Reflux	3 h	58
5	MNPs-DTPA-Cu (0.05)	H_2O	Reflux	3 h	30
6	MNPs-DTPA-Cu (0.05)	CH_3CN	Reflux	3 h	37
7	MNPs-DTPA-Cu (0.05)	n-Hexane	Reflux	3 h	<5
8	MNPs-DTPA-Cu (0.05)	-	50 °C	15 min	69
9	MNPs-DTPA-Cu (0.05)	-	80 °C	15 min	94
10	MNPs-DTPA-Cu (0.05)	-	100 °C	15 min	90
11	MNPs-DTPA-Cu (0.02)	-	80 °C	15 min	85
12	MNPs-DTPA-Cu (0.1)	-	80 °C	15 min	94
13	-	-	80 °C	4 h	<10
14	Fe_3O_4 (0.05)	-	80 °C	3 h	58

[a] Isolated yields.

To evaluate the catalyst's effectiveness, we performed a series of reactions involving *o*-phenylenediamine and various aldehydes. These aldehydes exhibited different characteristics, including electron-donating or electron-withdrawing groups, as well as diverse electronic structures and properties. The reactions were meticulously conducted under optimized conditions. The results of these experiments are presented in Table 2.

All reactions were efficiently carried out in the presence of catalytic amounts of MNPs-DTPA-Cu at a temperature of 80°C under solvent-free conditions. The desired products were obtained with high yields ranging from 83% to 96%. These results were achieved within relatively short reaction times, and notably, no side products such as imine intermediates, which are commonly observed, were formed. This demonstrates the effectiveness and selectivity of the catalyst in facilitating the desired transformations.

As indicated in Table 2, the process has been highly effective, and the nature of substituents on the aromatic ring of aldehydes significantly affected the performance and reaction time under the given conditions. Aldehydes bearing electron-withdrawing substituents exhibited superior yields and faster reaction times. Conversely, aldehydes featuring electron-donating groups displayed diminished efficiency.

Furthermore, the reaction with acid-sensitive aldehydes, such as thiophene-2-carbaldehyde and pyridine-2-carbaldehyde, resulted in the desired product with a good yield (Table 2, entries 5 and 10). However, the utilization

of certain aliphatic aldehydes, such as propionaldehyde and isobutyraldehyde, under the optimized reaction conditions, led to only minimal production of the corresponding product.

Table 2. Solvent-free synthesis of benzimidazoles by using MNPs-DTPA-Cu as the catalyst.

Entry	R	Product	Time (min)	Yield (%)[a]	M.P. (°C)	
					Found	Reported [Lit.]
1	C_6H_5	**3a**	15	94	294-296	296-298 [29]
2	4-ClC_6H_4	**3b**	12	95	295-296	298-300 [30]
3	4-$NO_2C_6H_4$	**3c**	15	93	301-302	303-304 [29]
4	4-MeC_6H_4	**3d**	20	91	274-276	275 [31]
5	2-Thienyl	**3e**	12	90	286-287	288-290 [32]
6	4-$MeOC_6H_4$	**3f**	30	88	220-222	221-223 [33]
7	4-HOC_6H_4	**3g**	30	85	225-227	229-230 [31]
8	4-$N(Me)_2C_6H_4$	**3h**	40	86	270-271	272-274 [33]
9	2-$MeOC_6H_4$	**3i**	35	85	182-183	181-182 [33]
10	2-Pyridyl	**3j**	15	83	241-243	245-248 [31]
11	2-ClC_6H_4	**3k**	25	89	232-234	232-233 [30]
12	3-$NO_2C_6H_4$	**3l**	15	96	201-203	203-205 [32]
13	3-Indolyl	**3m**	20	90	291-293	295-297 [34]
14	4-FC_6H_4	**3n**	20	92	246-247	248 [31]
15	2-Naphthyl	**3o**	25	91	217-219	218-219 [31]
16	2-HOC_6H_4	**3p**	40	86	235-236	236-237 [32]
17	3-HOC_6H_4	**3q**	40	88	272-273	275 [35]
18	2-6-$Cl_2C_6H_3$	**3r**	30	90	218-220	220 [35]
19	3-ClC_6H_4	**3s**	25	92	230-231	232-234 [31]
20	3,4,5-$(MeO)_3C_6H_2$	**3t**	30	89	256-257	259 [31]
21	2-$CO_2HC_6H_4$	**3u**	35	87	284-286	285-288 [30]
22	2-BrC_6H_4	**3v**	40	86	173-175	172 [36]

[a] Isolated yields.

A plausible mechanism for the formation of benzimidazole derivatives using the MNPs-DTPA-Cu catalyst, which supported by literature, is illustrated in Scheme 3. The presence of the copper cation in the catalyst allows it to act as a powerful Lewis acid, capable of coordinating with the carbonyl group. This coordination enhances the electrophilicity of the carbonyl atom, thereby promoting the reactivity of the aromatic aldehyde. As a result, the aldehyde can easily react with one NH_2 group of *o*-phenylenediamine, leading to the formation of Schiff's base.

With the aid of the nano-catalyst, the imine bond of the Schiff's base intermediate is attacked by the second amino group of o-phenylenediamine, leading to the formation of a five-membered ring through intramolecular ring closing. Subsequently, due to its high propensity for aromatization, this intermediate readily oxidizes in the presence of atmospheric oxygen, ultimately resulting in the formation of the benzimidazole product.

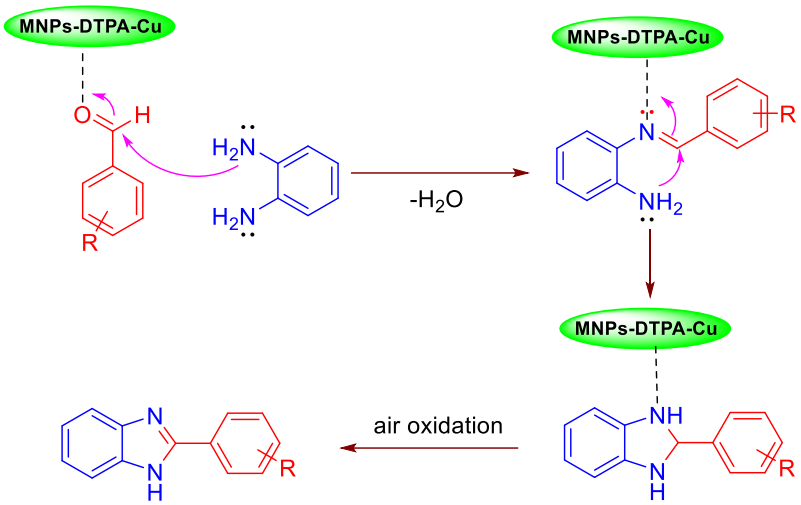

Scheme 3. Possible reaction mechanism for the synthesis of benzimidazole derivatives using MNPs-DTPA-Cu.

In order to assess the performance of the MNPs-DTPA-Cu catalyst, an extensive compilation of both organic and inorganic catalysts utilized for the synthesis of 2-phenyl-1H-benzo[d]imidazole under optimized conditions has been presented in Table 3. Furthermore, it is evident that the MNPs-DTPA-Cu catalyst not only possesses the general advantages associated with the inherent magnetic properties of nano-catalysts but also proves to be an equally or even more efficient catalyst for this particular reaction. Moreover, the MNPs-DTPA-Cu catalyst offers a range of additional benefits, including a short reaction time, straightforward conditions, environmental compatibility, high recoverability, ease of operation, and cost-effectiveness. These advantages collectively establish the MNPs-DTPA-Cu catalyst as an efficient choice for the synthesis of benzimidazole derivatives.

Table 3. Previously reported methods and catalyst for the formation of 2-phenyl-1H-benzo[d]imidazole [a]

Entry	Catalyst (amount)	Condition	Time	Yield (%)[b]	Ref.
1	I_2 (1 mmol)	DMF (35-40 °C)	4 h	81	[32]
2	CoO(II)(10 mol%)	EtOH (R.T.)	4 h	96	[34]
3	CuO-np/SiO_2 (10 mol%)	MeOH (R.T.)	4 h	93	[35]
4	$LaCl_3$ (10 mol%)	MeCN (R.T.)	3 h	88	[31]
5	Fe_3O_4 MNPs	EtOH (Reflux)	3 h	97	[37]
6	MNPs@Cu-PMT (20 mg)	EtOAc, 50°C	40 min	92	[30]
7	Nano-ZnO (10 mol%)	EtOH, Reflux	100 min	88	[38]
8	$Ce(NO_3)_3.6H_2O$ (30 mol%)	DMF, 800°C	90 min	93	[39]
9	Cu(II)–TD@nSiO_2(5mg)	Solvent-free (50 °C)	20 min	95	[40]
10	GO-VB1 (30 mg)	EtOH (R.T.)	35 min	90	[36]
11	PbO_2 (0.1 mmol)	Solvent-free, (R.T.)	10 min	94	[41]
12	MNPs-DTPA-Cu (0.05 g)	Solvent-free (80 °C)	15 min	94	This work

[a] Reaction conditions: *o*-phenylenediamine (1 mmol) and benzaldehyde (1 mmol).
[b] Isolated yields.

Catalyst recovery and reuse

The recovery and reusability of catalysts are pivotal in the field of chemistry and hold great importance for commercial and industrial applications. For this reason, extensive research has been conducted to explore the recovery and reusability of the MNPs-DTPA-Cu catalyst in the synthesis of 2-phenyl-1H-1,3-benzimidazole under optimized conditions. Upon completion of the reaction, the resultant solidified mixture was diluted with hot ethanol. Subsequently, the MNPs-DTPA-Cu catalyst was separated from the mixture using a powerful magnet and thoroughly washed with ethanol multiple times before being dried. The collected catalyst exhibited remarkable stability, as it was successfully employed in the subsequent reaction for six consecutive cycles without any notable decline in its catalytic activity. A summary of the outcomes from these reactions can be found in Fig. 8.

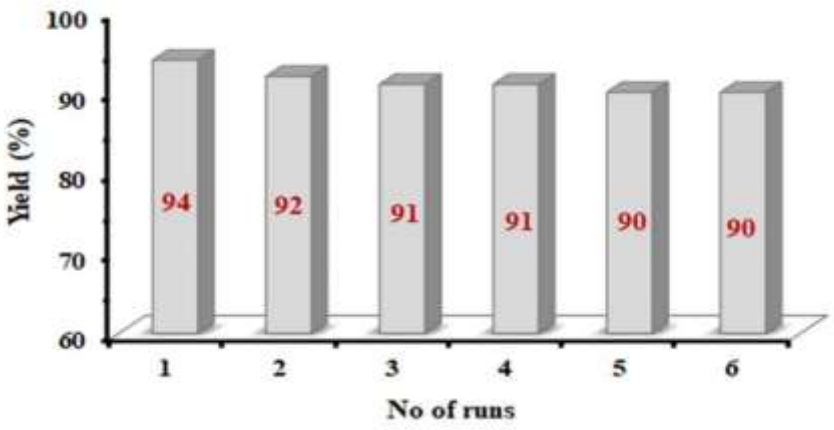

Fig. 8. The investigation of synthesized MNPs-DTPA-Cu recyclability for the model reaction under same reaction conditions.

4. Conclusions

In summary, a novel organic-inorganic magnetic nanocatalyst, known as MNPs-DTPA-Cu, has been successfully synthesized using a simple and cost-effective procedure. The formation and structure of this catalyst have been thoroughly investigated through the utilization of various advanced techniques, including FT-IR, XRD, TGA, FE-SEM, EDS, and VSM. The catalyst was effectively utilized in the one-pot reaction of *o*-phenylenediamine with aldehydes, conducted under solvent-free conditions. This reaction resulted in the production of benzimidazole derivatives with remarkable yields, reaching up to 96%. The high catalytic activity, broad applicability, high yield, short reaction time, and simple experimental procedure, along with easy product separation, make this method suitable and environmentally friendly for the synthesis of benzimidazole derivatives. Moreover, the catalyst exhibits remarkable stability under reaction conditions and can be easily separated by means of an external magnet. Notably, even after undergoing six cycles of utilization, it can be reused without any significant decrease in its catalytic activity.

Acknowledgment

The authors gratefully acknowledge the financial support and provision of experimental facilities by the Dezful Branch, Islamic Azad University.

References

[1] S. Bhattacharya, P. Chaudhuri, Medical implications of benzimidazole derivatives as drugs designed for targeting DNA and DNA associated processes, Current medicinal chemistry, 15 (18) 2008, 1762-1777. https://doi.org/10.2174/092986708785133013.
[2] B. Agrahari, S. Layek, R. Ganguly, N. Dege, D. D. Pathak, Synthesis, characterization and single crystal X-ray studies of pincer type Ni (II)-Schiff base complexes: Application in synthesis of 2-substituted benzimidazoles, Journal of Organometallic Chemistry, 890 2019, 13-20. https://doi.org/10.1016/j.jorganchem.2019.03.018.
[3] M. Nardi, N. C. H. Cano, S. Simeonov, R. Bence, A. Kurutos, R. Scarpelli, D. Wunderlin, A. Procopio, A review on the green synthesis of benzimidazole derivatives and their pharmacological activities, Catalysts, 13 (2) 2023, 392. https://doi.org/10.3390/catal13020392.
[4] S. M. Sondhi, N. Singh, A. Kumar, O. Lozach, L. Meijer, Synthesis, anti-inflammatory, analgesic and kinase (CDK-1, CDK-5 and GSK-3) inhibition activity evaluation of benzimidazole/benzoxazole derivatives and some Schiff's bases, Bioorganic & medicinal chemistry, 14 (11) 2006, 3758-3765. https://doi.org/10.1016/j.bmc.2006.01.054.
[5] S. Hameed P, A. Raichurkar, P. Madhavapeddi, S. Menasinakai, S. Sharma, P. Kaur, R. Nandishaiah, V. Panduga, J. Reddy, V. K. Sambandamurthy, Benzimidazoles: novel mycobacterial gyrase inhibitors from scaffold morphing, ACS Medicinal Chemistry Letters, 5 (7) 2014, 820-825. https://doi.org/10.1021/ml5001728.
[6] L. M. Dudd, E. Venardou, E. Garcia-Verdugo, P. Licence, A. J. Blake, C. Wilson, M. Poliakoff, Synthesis of benzimidazoles in high-temperature water, Green Chemistry, 5 (2) 2003, 187-192. https://doi.org/10.1039/B212394K.
[7] J. G. Smith, I. Ho, Organic redox reactions during the interaction of o-phenylenediamine with benzaldehyde, Tetrahedron Letters, 12 (38) 1971, 3541-3544. https://doi.org/10.1016/S0040-4039(01)97226-0.
[8] M. P. Singh, S. Sasmal, W. Lu, M. N. Chatterjee, Synthetic utility of catalytic Fe (III)/Fe (II) redox cycling towards fused heterocycles: a facile access to substituted benzimidazole, bisbenzimidazole and imidazopyridine derivatives, Synthesis, 2000 (10) 2000, 1380-1390. https://doi.org/10.1055/s-2000-7111.
[9] R. Trivedi, S. K. De, R. A. Gibbs, A convenient one-pot synthesis of 2-substituted benzimidazoles, Journal of Molecular Catalysis A: Chemical, 245 (1-2) 2006, 8-11. https://doi.org/10.1016/j.molcata.2005.09.025.
[10] M. A. Chari, P. Sadanandam, D. Shobha, K. Mukkanti, A simple, mild, and efficient procedure for high-yield synthesis of benzimidazoles using coppertriflate as catalyst, Journal of Heterocyclic Chemistry, 47 (1) 2010, 153-155. https://doi.org/10.1002/jhet.287.
[11] R. Nagawade, D. Shinde, Zirconyl (IV) chloride-promoted synthesis of benzimidazole derivatives, Russian journal of organic chemistry, 42 2006, 453-454. https://doi.org/10.1134/S1070428006030201.
[12] V. R. Ruiz, A. Corma, M. J. Sabater, New route for the synthesis of benzimidazoles by a one-pot multistep process with mono and bifunctional solid catalysts, Tetrahedron, 66 (3) 2010, 730-735. https://doi.org/10.1016/j.tet.2009.11.048.
[13] P. Gogoi, D. Konwar, An efficient and one-pot synthesis of imidazolines and benzimidazoles via anaerobic oxidation of carbon–nitrogen bonds in water, Tetrahedron letters, 47 (1) 2006, 79-82. https://doi.org/j.tetlet.2005.10.134.
[14] H. Göker, C. Kuş, D. W. Boykin, S. Yildiz, N. Altanlar, Synthesis of some new 2-substituted-phenyl-1H-benzimidazole-5-carbonitriles and their potent activity against Candida species, Bioorganic & medicinal chemistry, 10 (8) 2002, 2589-2596. https://doi.org/10.1016/S0968-0896(02)00103-7.
[15] P. Salehi, M. Dabiri, M. A. Zolfigol, S. Otokesh, M. Baghbanzadeh, Selective synthesis of 2-aryl-1-arylmethyl-1H-1, 3-benzimidazoles in water at ambient temperature, Tetrahedron Letters, 47 (15) 2006, 2557-2560. https://doi.org/10.1016/j.tetlet.2006.02.049.
[16] L.-H. Du, Y.-G. Wang, A rapid and efficient synthesis of benzimidazoles using hypervalent iodine as oxidant, Synthesis, 2007 (05) 2007, 675-678. https://doi.org/10.1055/s-2007-965922.
[17] K. Tanaka, F. Toda, Solvent-free organic synthesis, Chemical Reviews, 100 (3) 2000, 1025-1074. https://doi.org/10.1021/cr940089p.
[18] S. Laurent, D. Forge, M. Port, A. Roch, C. Robic, L. Vander Elst, R. N. Muller, Magnetic iron oxide nanoparticles: synthesis, stabilization, vectorization, physicochemical characterizations, and biological applications, Chemical reviews, 108 (6) 2008, 2064-2110. https://doi.org/10.1021/cr068445e.
[19] S. K. Bagaria, N. Jangir, D. K. Jangid, Green and eco-compatible iron nanocatalysed synthesis of benzimidazole: A review, Sustainable Chemistry and Pharmacy, 31 2023, 100932. https://doi.org/10.1016/j.scp.2022.100932.
[20] H. Moghanian, M. A. B. Fard, A. Mobinikhaledi, N. Ahadi, Bis (p-sulfoanilino) triazine-functionalized silica-coated magnetite nanoparticles as an efficient and magnetically reusable nano-catalyst for Biginelli-type reaction, Research on Chemical Intermediates, 44 (7) 2018, 4083-4101. https://doi.org/10.1007/s11164-018-3357-5.

[21] M. B. Gawande, P. S. Branco, R. S. Varma, Nano-magnetite (Fe_3O_4) as a support for recyclable catalysts in the development of sustainable methodologies, Chemical Society Reviews, 42 (8) 2013, 3371-3393. https://doi.org/10.1039/C3CS35480F.
[22] S. M. Patil, R. Tandon, N. Tandon, I. Singh, A. Bedre, V. Gade, Magnetite-supported montmorillonite (K10)(nanocat-Fe-Si-K10): an efficient green catalyst for multicomponent synthesis of amidoalkyl naphthol, RSC advances, 13 (25) 2023, 17051-17061. https://doi.org/10.1039/D3RA01522J.
[23] S. Liu, B. Yu, S. Wang, Y. Shen, H. Cong, Preparation, surface functionalization and application of Fe_3O_4 magnetic nanoparticles, Advances in colloid and Interface Science, 281 2020, 102165. https://doi.org/10.1016/j.cis.2020.102165.
[24] N. Tran, T. J. Webster, Magnetic nanoparticles: biomedical applications and challenges, Journal of Materials Chemistry, 20 (40) 2010, 8760-8767. https://doi.org/10.1039/C0JM00994F.
[25] K. Can, M. Ozmen, M. Ersoz, Immobilization of albumin on aminosilane modified superparamagnetic magnetite nanoparticles and its characterization, Colloids and Surfaces B: Biointerfaces, 71 (1) 2009, 154-159. https://doi.org/10.1016/j.colsurfb.2009.01.021.
[26] V. Fomenko, T. Polynova, M. Porai-Koshits, G. Varlamova, N. Pechurova, Crystal structure of copper (II) diethylenetriaminepentaacetate monohydrate, Journal of Structural Chemistry, 14 (3) 1973, 529-529. https://doi.org/10.1007/BF00747020.
[27] J. Giri, S. G. Thakurta, J. Bellare, A. K. Nigam, D. Bahadur, Preparation and characterization of phospholipid stabilized uniform sized magnetite nanoparticles, Journal of magnetism and magnetic materials, 293 (1) 2005, 62-68. https://doi.org/10.1016/j.jmmm.2005.01.044.
[28] K. Petcharoen, A. Sirivat, Synthesis and characterization of magnetite nanoparticles via the chemical co-precipitation method, Materials Science and Engineering: B, 177 (5) 2012, 421-427. https://doi.org/10.1016/j.mseb.2012.01.003.
[29] D. Xue, Y.-Q. Long, Metal-free TEMPO-promoted C(sp3)–H amination to afford multisubstituted benzimidazoles, The Journal of Organic Chemistry, 79 (10) 2014, 4727-4734. https://doi.org/10.1021/jo5005179.
[30] A. Mobinikhaledi, H. Moghanian, S. M. B. H. Ghazvini, A. Dalvand, Copper containing poly(melamine-terephthaldehyde)-magnetite mesoporous nanoparticles: a highly active and recyclable catalyst for the synthesis of benzimidazole derivatives, Journal of Porous Materials, 25 (4) 2018, 1123-1134. https://doi.org/10.1007/s10934-017-0524-9.
[31] Y. Venkateswarlu, S. R. Kumar, P. Leelavathi, Facile and efficient one-pot synthesis of benzimidazoles using lanthanum chloride, Organic and Medicinal Chemistry Letters, 3 (1) 2013, 1-8. https://doi.org/10.1186/2191-2858-3-7.
[32] S. Ponnala, D. Prasad Sahu, Iodine-mediated synthesis of 2-arylbenzoxazoles, 2-arylbenzimidazoles, and 1,3,5-trisubstituted pyrazoles, Synthetic Communications, 36 (15) 2006, 2189-2194. https://doi.org/10.1080/00397910600638879.
[33] C. Chen, C. Chen, B. Li, J. Tao, J. Peng, Aqueous synthesis of 1-h-2-substituted benzimidazoles via transition-metal-free intramolecular amination of aryl iodides, Molecules, 17 (11) 2012, 12506-12520. https://doi.org/10.3390/molecules171112506.
[34] M. Adharvana Chari, D. Shobha, T. Sasaki, Room temperature synthesis of benzimidazole derivatives using reusable cobalt hydroxide (II) and cobalt oxide (II) as efficient solid catalysts, Tetrahedron Letters, 52 (43) 2011, 5575-5580. https://doi.org/10.1016/j.tetlet.2011.08.047.
[35] S. M. Inamdar, V. K. More, S. K. Mandal, CuO nano-particles supported on silica, a new catalyst for facile synthesis of benzimidazoles, benzothiazoles and benzoxazoles, Tetrahedron Letters, 54 (6) 2013, 579-583. https://doi.org/10.1016/j.tetlet.2012.11.091.
[36] H. Ghafuri, N. Joorabchi, A. Emami, H. R. Esmaili Zand, Covalent modification of graphene oxide with vitamin B1: preparation, characterization, and catalytic reactivity for synthesis of benzimidazole derivatives, Industrial & Engineering Chemistry Research, 56 (22) 2017, 6462-6467. https://doi.org/10.1021/acs.iecr.7b00182.
[37] A. Sajjadi, R. Mohammadi, Fe_3O_4 magnetic nanoparticles (fe_3o_4 mnps): A magnetically reusable catalyst for synthesis of benzimidazole compounds, Journal of Medicinal and Chemical Sciences, 2 (2) 2019, 41-75. https://doi.org/10.26655/jmchemsci.2019.3.4.
[38] A. Teimouri, A. N. Chermahini, H. Salavati, L. Ghorbanian, An efficient and one-pot synthesis of benzimidazoles, benzoxazoles, benzothiazoles and quinoxalines catalyzed via nano-solid acid catalysts, Journal of Molecular Catalysis A: Chemical, 373 2013, 38-45. https://doi.org/10.1016/j.molcata.2013.02.030.
[39] G. M. Martins, T. Puccinelli, R. A. Gariani, F. R. Xavier, C. C. Silveira, S. R. Mendes, Facile and efficient aerobic one-pot synthesis of benzimidazoles using $Ce(NO_3)_3{\cdot}6H_2O$ as promoter, Tetrahedron Letters, 58 (20) 2017, 1969-1972. https://doi.org/10.1016/j.tetlet.2017.04.020.
[40] M. Zakeri, M. Moghadam, V. Mirkhani, S. Tangestaninejad, I. Mohammadpoor-Baltork, Z. Pahlevanneshan, Copper containing nanosilica thioalated dendritic material: A recyclable catalyst for synthesis of benzimidazoles and benzothiazoles, Applied Organometallic Chemistry, 32 (1) 2018, e3937. https://doi.org/10.1002/aoc.3937.
[41] V. D. Patil, J. Patil, P. Rege, G. Dere, Mild and efficient synthesis of benzimidazole using lead peroxide under solvent-free conditions, Synthetic Communications, 41 (1) 2010, 58-62. https://doi.org/10.1080/00397910903531789.